Available online at www.sciencedirect.com
ScienceDirect
Journal of Photochemistry and Photobiology A: Chemistry 190 (2007) 22–28
Journal of Photochemistry and Photobiology A:Chemistry
www.elsevier.com/locate/jphotochem

Two-photon photopolymerization using novel asymmetric ketocoumarin derivatives

Xue Li, Yuxia Zhao *, Jie Wu, Mengquan Shi, Feipeng Wu **

Technical Institute of Physics and Chemistry, Chinese Academy of Sciences, Beijing 100080, PR China

Received 13 November 2006; received in revised form 9 February 2007; accepted 6 March 2007

Abstract

A series of stilbene modified asymmetric ketocoumarin derivatives (compounds **1**–**4**) with varied electron-donating terminal groups used on two-photon photopolymerization were reported. Solvatochromism analysis showed that the compounds with strong electron-donating terminal groups exhibited larger dipole moment change than those with weak electron-donating groups upon excitation. In addition, these compounds with strong electron-donating groups presented excellent two-photon absorption properties. Their two-photon absorption cross-sections are two magnitudes larger than those of common UV–vis sensitive photosensitizers. The results of photobleaching and one-photon polymerization experiments also showed that these compounds had high photoactivity on photosensitized photolysis of *o*-chloro hexaarylbiimidazoles (*o*-Cl-HABI) and 4,4′-dimethyldiphenyliodinium hexafluorophosphate (DPI) to generate radicals. As an example, the combination of compound **4** with *o*-Cl-HABI, an efficient two-photon photopolymerization initiation system, has been preliminarily demonstrated for fabrication of 3D micro-structures.

Keywords: Two-photon absorption; Two-photon photopolymerization; Ketocoumarin

1. Introduction

Two-photon photopolymerization (TPP) is a powerful technique for fabrication of three-dimensional (3D) micro- and submicro-structures. The photoinitiation system for TPP is excited by simultaneous absorption of two photons leading to chemical polymerization reactions. Due to a tight confinement of the excitation volume around the focal point, this method can produce micrometer sized and highly resolved objects. The production of high-fidelity micro-structures having complex 3D form and feature sizes as small as 100–200 nm has demonstrated the potential application of this approach in optical devices [1–3], optical storage [4], photonic bandgaps [5,6] and micromachines [7,8]. As one of important components of the polymerization system, a highly efficient photoinitiation system requires both a large two-photon absorption cross-section (δ) and a high efficiency to create reactive species after photolysis. The quantum yield and the activity of species produced by photoinitiation system are significant to decrease the threshold of polymerization, minimize the damage of materials and reduce the polymerization cost. At present, most work in the field has involved patterning structures in commercial acrylate resins using conventional UV-active initiators [9–11]. The conventional UV-active initiators have high initiation efficiency but low two-photon absorption ability [12], so high excitation power and long exposure time are needed to cure the resin, which often result in damage to the structure. This aspect is an obstacle for the versatility of TPP and its widespread applications. New initiators that display strong two-photon absorption together with good initiation efficiency are required for achieving low power and short time of exposure.

Ketocoumarin dyes are well-known highly efficient photosensitizers and photoinitiators in UV–vis curable systems [13,14]. Photosensitive systems based on a mixture of ketocoumarins with amino, iron arene complex, iodonium and biimidazoles have been widely investigated [15–19]. Given improved δ, they are liable to be highly efficient photosensitizers or photoinitiators for two-photon polymerization in NIR region [20]. So in this paper, a series of stilbene modified asymmetric ketocoumarin derivatives with a variety of terminal substituted groups were reported. The one- and two-photon photophysical

---

* Corresponding author. Tel.: +86 10 82543571; fax: +86 10 82543569.
** Corresponding author.
E-mail address: yuxia.zhao@mail.ipc.ac.cn (Y. Zhao).

1010-6030/$ – see front matter © 2007 Elsevier B.V. All rights reserved.
doi:10.1016/j.jphotochem.2007.03.007

properties of these compounds were investigated systematically by UV–vis spectra, steady-state fluorescence spectra, and two-photon excited fluorescence (TPEF) technique with femtosecond laser pulses. The solvatochromic behaviors of these compounds were studied, which might provide information on understanding the structure–property relationships. The photosensitization efficiency of these compounds was evaluated by simple and convenient photobleaching and one-photon polymerization experiments. Finally, two-photon photopolymerization was performed.

2. Experimental

2.1. Materials

Compounds **1**–**4** (Scheme 1) were synthesized by Knoevenagel reactions, Aldol condensations and Wittig reactions with high yields. The detailed synthesis process was described elsewhere [21]. Epoxy diacrylate oligomer (CN124A80), pentaerythritol triacrylate (SR444), 2-phenoxyethyl acrylate esters (SR339) were all from Sartomer and used as received. *o*-Chloro hexaarylbiimidazoles (*o*-Cl-HABI) was from Tokyo Kasei Kogyo Co. Ltd. 4,4′-Dimethyldiphenyliodinium hexafluorophosphate (DPI) was from TH-UNIS Insight Co. Ltd. *N*-Phenyl glycine (NPG) was from Acros. Biscoumarin (**R**) was synthesized in our lab according to the literature [13]. The structures of *o*-Cl-HABI, DPI, NPG and **R** are illustrated in Scheme 2. Other reagents (A.R.) were all from Beijing Beihua Co. Ltd. and used after purifications with common methods.

2.2. Methods

UV–vis spectra were recorded on a Jasco V-530 spectrophotometer. Steady-state fluorescence measurements were performed at room temperature using a Hitachi F-4500 spectrometer. Fluorescence quantum yields were measured in diluted solutions (10^{-6} M) using fluorescein in 0.1N NaOH as a standard ($\Phi = 0.90$) and refractive index correction was performed [22]. Two-photon absorption cross-sections of all compounds in chloroform solution (10^{-4} to 10^{-3} M) were determined using two-photon excited fluorescence technique with femtosecond laser pulses (from a Tsunami mode-locked Ti: sapphire, 695–880 nm, 80 MHz, <130 fs) following the experimental protocol described in detail by Xu and Webb [23]. Fluorescein in 0.1N NaOH (10^{-4} M) and Rhodamine B in methanol solution (10^{-4} M) were used as references to calibrate our measurement. The δ of compounds was calculated according to the following equation:

$$\delta_s = \frac{S_s \Phi_r \varphi_r c_r}{S_r \Phi_s \varphi_s c_s} \delta_r \qquad (1)$$

where the subscripts s and r stand for the sample and reference molecules. S is the integral area of the two-photon excited fluorescence, Φ is the fluorescence quantum yield, φ is the overall fluorescence collection efficiency of the experimental apparatus, and c is the number density of the molecules in solution. The experimental errors are within range of ±15%.

Photobleaching was performed in acetonitrile solutions and the solutions were deoxygenated by bubbling with high purity nitrogen. The light source was a 400 W Xenon lamp. The intensity of irradiation was 20 mW/cm^2.

In one-photon polymerization experiments, the resin was consisted of CN124A80, SR444 and SR339 (m_{CN124A80}:m_{SR444}:m_{SR339} = 3:5:1). The mass ratios of photosensitizer and photoinitiator to the resin were 0.08% and 1%, respectively. *N*-Phenylglycine (NPG) was used as coinitiator and the mass ratio of NPG to the resin was 1%. After the photosensitizer, photoinitiator and coinitiator dissolving in the mixed solvent of dichloromethane and methanol (m:m = 9:1), they were blended with the resin. The mixed solution was poured into a glass cell made in our laboratory. The thickness of the sample was 0.5 mm. The light source was an EFOS Lite 50 W miniature arc lamp with 5 mm crystal optical fiber. A band-pass filter was inserted and only light of 400–500 nm irradiated on the sample. The disappearance of double bonds during the photocuring of the formulation was recorded by real-time Fourier transform infrared (RT-FTIR) spectroscopy (Nicolet Magna 5700 real-time FTIR). Infrared spectra were collected with Nicolet data processing software series 7.1. In all cases, three kinetic runs were carried out to verify reproducibility for each photopolymerization studied.

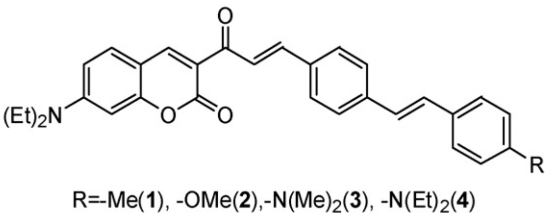

Scheme 1. Structures of compounds **1**–**4**.

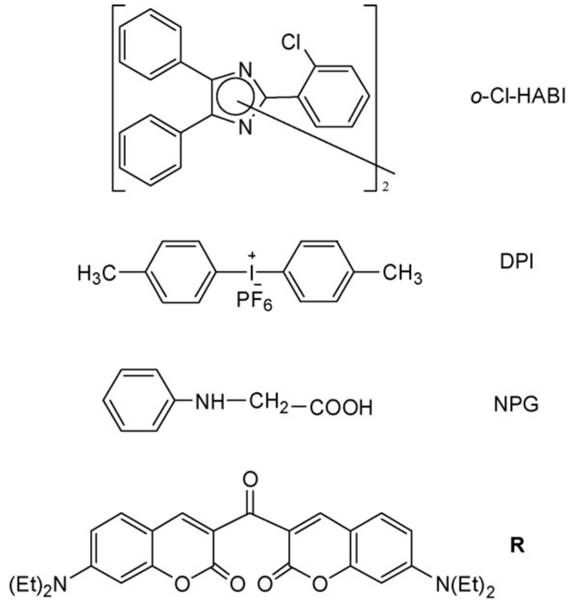

Scheme 2. Structures and abbreviated formula of the photoinitiators, coinitiator and reference compound.

Two-photon photopolymerization experiments were performed using the same laser used in TPEF measurement. The laser was focused through a 40× objective lens with a numerical aperture (NA) of 0.45. The samples were placed on a three axis piezoelectric stage (P-762.3L nanopositioner) controlled by a computer. The resin used in two-photon photopolymerization was same as that used in one-photon photopolymerization. The polymerization films with a thickness of 200–300 μm were obtained by spin-coating the resin on a glass slide. After two-photon photopolymerization, the polymerized structures were easily obtained by developing in acetone. Scanning electron microscopy (SEM) images were obtained using a Hitachi S-4300F SEM.

3. Results and discussion

3.1. One-photon optical properties

The UV–vis absorption spectra and steady-state fluorescence spectra of compounds **1–4** in chloroform are shown in Fig. 1. The linear absorption maxima of these compounds exist at around 470 nm. The one-photon absorption peaks have a slight red-shift with the change of terminal substituted groups in the order of –Me$_2$N (**3**) > –Et$_2$N (**4**) > –MeO (**2**) > –Me (**1**). Whereas the fluorescence spectra display a systematic bathochromic shift with the increase of electron-donating strength of the terminal substituted groups from –Me (**1**), –OMe (**2**) to –NMe$_2$ (**3**), –NEt$_2$(**4**). Compounds **3** and **4** show much larger value of Stokes shifts in comparison to **1** and **2**, indicating that their energy gap between their ground and their lowest excited state decreases as their donor strength increases, and their lowest excited states are more likely to be a charge transfer state.

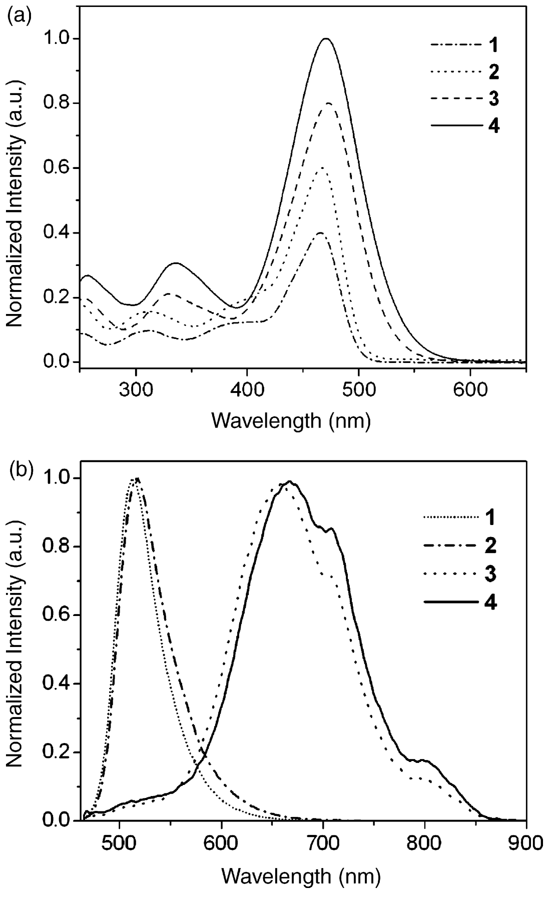

Fig. 1. Normalized one-photon absorption (a) and normalized fluorescence spectra excited at 460 nm (b) of compounds **1–4** in chloroform.

The distance of intramolecular charge transfer along the π-bridge of compounds upon excitation could be characterized by determining the dipole moment change. The dipole moment change ($\Delta\mu$) of the compounds in the solution phase can be estimated by solvatochromism analysis. To further quantificationally evaluate the extent of charge transfer of compounds **1–4** upon excitation, we measured the solvent effect of the four compounds. The photophysical properties of the compounds in different polarity solvents are listed in Table 1. According to Lippert–Mataga equation [24], the dipole moment change can be obtained from the plot of Stokes shift ($\Delta\upsilon_{ss}$) as a function of the orientational polarizability (Δf) of the solvent:

$$\Delta\upsilon_{ss} = \frac{2\Delta\mu^2\Delta f}{hca^3} + \text{const.} \tag{2}$$

In the equation, h is the Planck constant, c is the light velocity, a is the radius of the solute spherical cavity, and Δf is defined as

$$\Delta f = \frac{\varepsilon - 1}{2\varepsilon + 1} - \frac{n^2 - 1}{2n^2 + 1} \tag{3}$$

where ε is the dielectric constant and n is the refractive index of the solvent. The Lippert plots for the four compounds are illustrated in Fig. 2. There was no significant deviation from the linearity. The value of a is dependent on the length of a molecule. For the four compounds with similar structures, the length of them can be estimated to be equal. So the slope ($2\Delta\mu^2/hca^3$) of the Lippert plots represents the $\Delta\mu^2$ of the compounds. The calculated solvatochromic slopes from the linear fitting of experimental data are 6845 (**1**), 6618 (**2**), 17,746 (**3**) and 17,608 (**4**). The $\Delta\mu^2$ of compounds **3** and **4** are nearly three times that of compounds **1** and **2**. It is an indication that greater π-electron

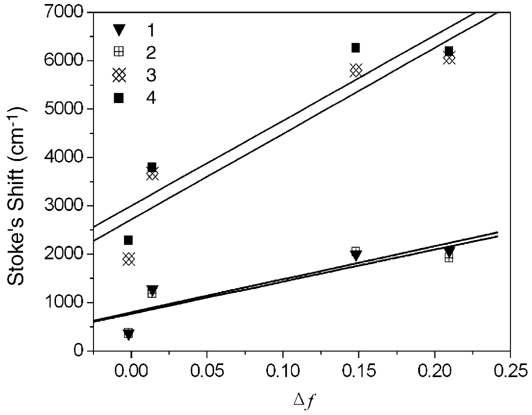

Fig. 2. Lippert–Mataga correlations for compounds **1–4**.

Table 1
Photophysical data of compounds **1**–**4** in different solvents

Compounds	Solvents	λ^{a}_{max} (nm)	$\lg \varepsilon_{max}$	λ^{f}_{max} (nm)	$\Delta\upsilon_{ss}$ (cm^{-1})	Φ_f	δ_{max} (GM)	λ^{TPA}_{max} (nm)
1	Cyclohexane	446.5	4.13	454	370			
	Toluene	458.5	4.84	487	1280			
	THF	460.5	4.90	509	2070			
	Chloroform	466	4.90	514	2000	0.31	332	800
2	Cyclohexane	447.5	3.75	455	368			
	Toluene	459.5	4.80	486	1190			
	THF	462	4.80	507	1920			
	Chloroform	467.5	4.98	517	2050	0.40	318	800
3	Cyclohexane	450	3.67	492	1900			
	Toluene	464.5	4.85	560	3670			
	THF	469.5	4.90	633	6060			
	Chloroform	473	4.93	652	5800	0.023	1570	850
4	Cyclohexane	448	4.43	499	1180			
	Toluene	464	4.83	564	3790			
	THF	467.5	4.85	658	6190			
	Chloroform	471.5	4.89	669	6260	0.015	1349	880

λ^{a}_{max}: one-photon absorption maxima in nm, $\lg \varepsilon_{max}$: logarithm of maximum molar absorption coefficient, λ^{f}_{max}: one-photon induced fluorescence maxima in nm, $\Delta\upsilon_{ss}$: Stoke's shifts in cm^{-1}, Φ_f: fluorescence quantum yield. δ_{max}: the maximum two-photon absorption cross-section in GM (1 GM = 10^{-50} cm^4 s photon^{-1}) within measured range, λ^{TPA}_{max}: the wavelength that the maximum two-photon absorption cross-section located at.

delocalization through intramolecular charge transfer occurred during excitation leading to larger polarizability, which is an important factor directly related to the nonlinear absorption property of compounds [25–28].

3.2. Two-photon absorption

The two-photon absorption cross-sections of compounds **1**–**4** were measured using the TPEF method. The results are shown in Fig. 3. Because the TPEF spectra of compounds **3** and **4** had a part of overlap with the residual excitation light when the excited wavelength was shorter than 850 nm, only their two-photon excited spectra between 850 and 880 nm were determined, while the δ of compounds **1** and **2** between 720 and 880 nm were measured. The largest δ of compounds **3** and **4** were obtained as 1570 and 1349 GM within the studied spectral region, respectively. For compounds **1** and **2**, the two-photon absorption spectra showed a maximum in 800 nm, and the values were 332 and 318 GM, respectively. Obviously, the change of terminal groups from –Me (**1**), –OMe (**2**) to –N(Me)$_2$ (**3**), –N(Et)$_2$ (**4**) had an significant effect on the two-photon absorption cross-section. The δ of compounds **3** and **4** were much larger than that of compounds **1** and **2** and two magnitudes larger than that of the common UV–vis sensitive photosensitizers [29,30]. Thus the dramatic increase of δ were achieved by increasing the electron-donating ability of terminal group. This observation was consisted with the aforementioned solvatochromic behavior of the four compounds.

Herein, it should be noteworthy that one-photon fluorescence spectra and two-photon fluorescence spectra of compounds **1** and **3** exhibited similar shape and peak wavelength as shown in Fig. 4, which indicated that they emitted from the same level of excited states. Compounds **2** and **4** had the same properties (not shown here).

3.3. Photosensitizing efficiencies

On the basis of the facts that the emission spectra excited by one-photon or two-photon of the compounds studied here are

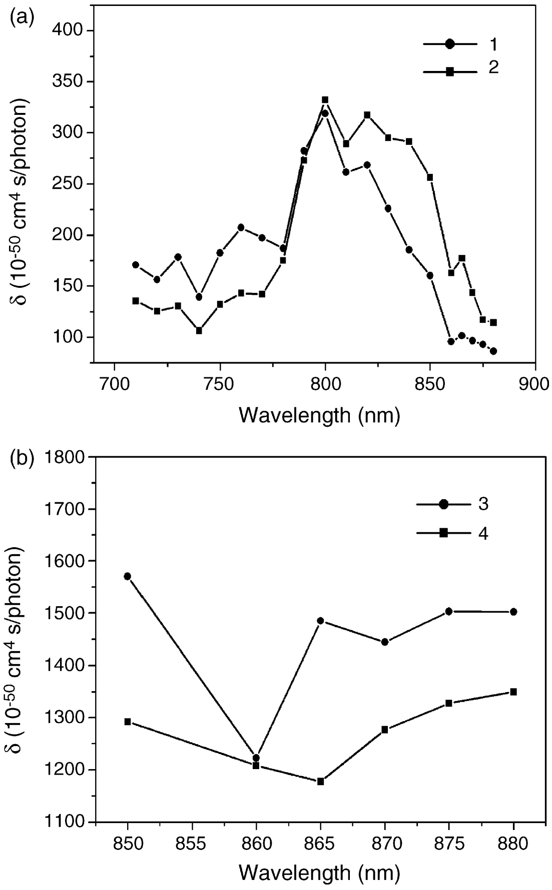

Fig. 3. Two-photon absorption cross-sections of compounds **1**–**4** in chloroform.

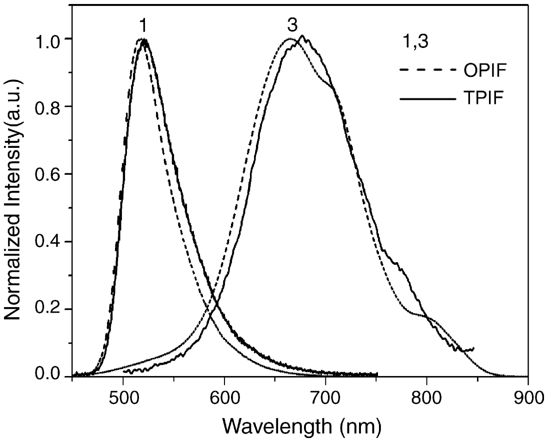

Fig. 4. One-photon excited fluorescence and two-photon excited fluorescence of compounds **1** and **3** in chloroform.

same, it may be considered that their photoreaction excited state is at the same level. So we can conveniently use one-photon absorption process to evaluate the photosensitizing efficiencies of compounds in TPP. Considering the excellent two-photon properties of compounds **3** and **4**, the photosensitizing systems are consisted of compound **3** or **4** and photoinitiator *o*-Cl-HABI (a well-known radical source). Because the photoinduced electron transfer from dyes to *o*-Cl-HABI leads to a remarkable dye photobleaching, the photoreaction kinetic study can be carried out by monitoring the relative change in optical density $((OD_0 - OD_t)/OD_0)$ of the absorption peak of dyes with the irradiation time, where OD_0 and OD_t are the optical density of the absorption peak of dyes before and after irradiation, respectively. The spectral changes of dye/*o*-Cl-HABI system in acetonitrile with the irradiation time are shown in Fig. 5 and their photobleaching rate plots are shown in Fig. 6. A fast decrease in absorption was observed upon irradiation and rapidly reached to a plateau about 60%. Under the same experimental condition, the absorption of compounds **3** and **4** alone did not change after irradiation. So this spectra change can be attributed to the photoinduced electron transfer from dyes to *o*-Cl-HABI. Thus compounds **3** and **4** are both effective photosensitizers for photolysis of *o*-Cl-HABI.

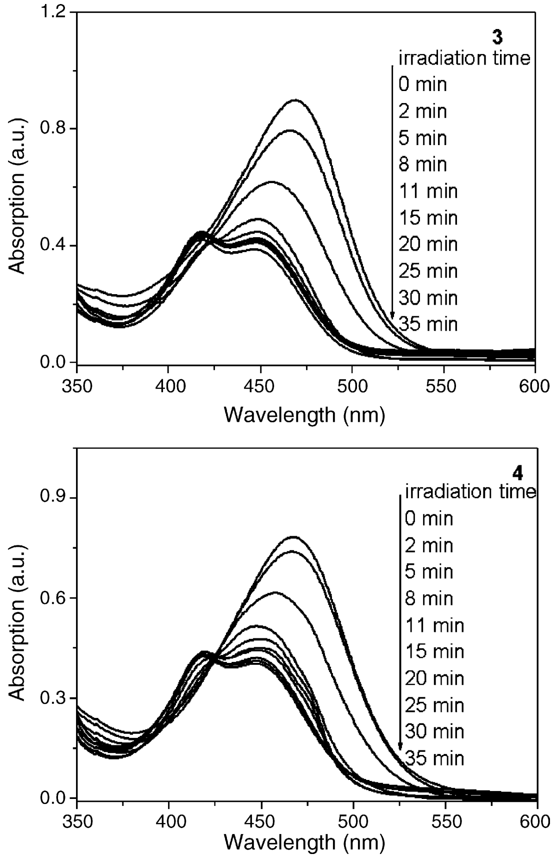

Fig. 5. Spectral changes by irradiation of acetonitrile solution of compounds **3** and **4**/*o*-Cl-HABI.

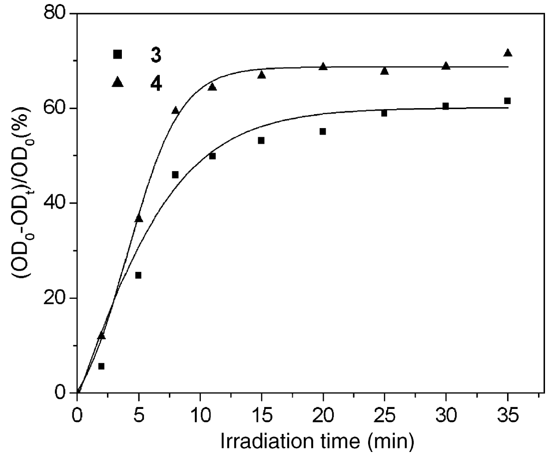

Fig. 6. Photobleaching rates of compounds **3** and **4**/*o*-Cl-HABI system in acetonitrile (the solid line is a guide to the eye).

Diaryliodonium is another important kind of photoinitiator which can photoinitiate cationic and radical polymerization. So it is of considerable interest to construct a new photosensitizing system of diaryliodonium with compound **3** or **4**. The photosensitizing efficiencies of compounds **3** and **4** on the photolysis of diaryliodonium and subsequent initiating polymerization were detected and assessed by employing real-time Fourier transfer infrared spectroscope which is a useful method to monitor the kinetics of rapid photopolymerization reactions and probe these types of reactions [31–33]. By recording the relative changes of

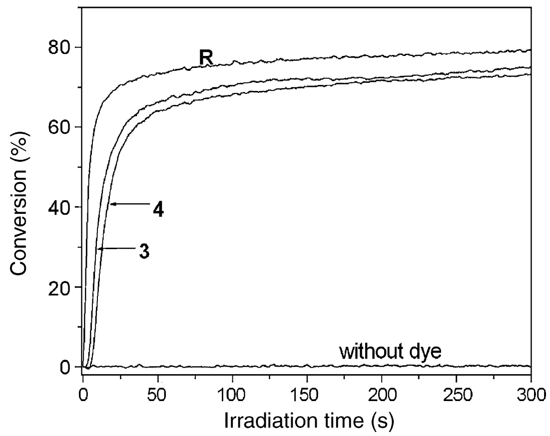

Fig. 7. FT-RTIR comparison of the polymerization of acrylate in the presence of dye/DPI/NPG.

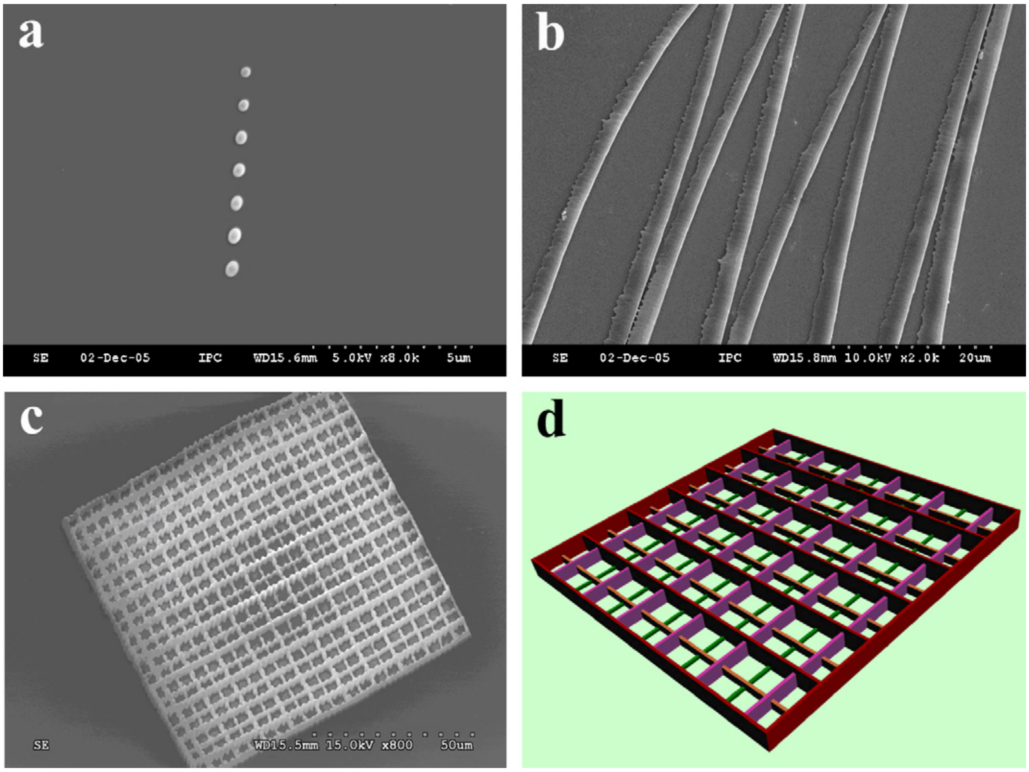

Fig. 8. Scanning electron microscopy images of the polymerized structures by two-photon photopolymerization with photosentizing system **4**/*o*-Cl-HABI. Excitation wavelength: 800 nm; laser power: 4 mW; scanning rate: 50 μm/s. (a) Polymerized dots; (b) polymerized lines; (c) polymerized 3D periodical lattice; (d) the model of the 3D periodical lattice.

the double bond absorption of acrylate monomers at 6164 cm^{-1} in the near infrared region, it allows the direct determination of the photosensitizing efficiencies of different dyes [34]. In our experiment, the well-known efficient photosensitizer biscoumarin (**R**) was used as a reference photosensitizer [32]. A comparison of the polymerization of acrylate resin in the presence and absence of photosensitizer is shown in Fig. 7. In the absence of photosensitizer, there was no polymerization happened even after irradiation for 300 s. However, in the presence of photosensitizer, polymerization underwent readily and the polymerization rate was comparable with the value of biscoumarin (**R**). Within the range of 30 s, the photosensitized polymerizations completed and conversion curves reached to their plateau. This implies that compounds **3** and **4** used for photosensitized photolysis of DPI were comparable with the reference compound **R**.

Based on the results obtained from the photosensitized primary photoreaction and subsequent polymerization, it can be considered that compounds **3** and **4** are useful photosensitizers for construction of an active photosensitization system in combination with suitable photoinitiators such as *o*-Cl-HABI and DPI.

3.4. *Two-photon photopolymerization*

To demonstrate the performance of the studied compounds in two-photon photopolymerization, compound **4**/*o*-Cl-HABI combination was used as photoinitiating system to initiate two-photon polymerization of acrylates. The polymerized dots, lines and periodical 3D structures were easily obtained by developing in acetone. The scanning electronic microscopy images of the polymerized structures are shown in Fig. 8. The dots were obtained by exposing different time and the size increased with the increase of exposure time. The width of the lines is 2.5 μm. In the periodical structure, the size of every grid is 5 μm × 5 μm and the heights of four walls are 2.5, 2, 1.5 and 1 μm. Although it was relatively difficult to give precise threshold of polymerization because of the lack of a standard method to measure the focal spot power of polymerization which related to the repetition frequency, pulse width, size of the focal point and so on, it was observed that the polymerization occurred rapidly at the average power of 4 mW measured before lens. This value is lower than that of the common UV–vis sensitized photoinitiators used in TPP [10,35]. This highly efficient two-photon photoinitiation system might be due to (1) the greatly increased two-photon absorption cross-section of the photosensitizer and (2) the high ability of electron transfer from photosensitive dye to the initiator leading to efficient generation of reactive species.

4. Conclusions

In this work, we have reported the linear photophysical, photochemical behaviors and the two-photon properties of a series of stilbene modified asymmetric ketocoumarin derivatives systematically. The compounds substituted by strong electron-donating terminal groups displayed large polarizability upon excitation as resulted from the solvatochromic analysis and exhibited large δ determined by TPEF method. The maximum two-photon absorption cross-sections obtained with femtosecond laser pulses was 1570 GM. These compounds also displayed efficient photosensitive activity on photolysis of the suitable photoinitiator such as *o*-Cl-HABI and DPI to initiate radical polymerization. In addition, two-photon photopolymerization using compound **4**/*o*-Cl-HABI as the photosensitive system was carried out. Periodical 3D micro-structures were obtained easily at lower excitation power. The present results are very useful for the practical application of two-photon photopolymerization.

Acknowledgements

This work was supported by financial support from the National Science Foundation of China (50403030 and 60477004). We thank Ms. Xiangyun Fang for her help on TPEF measurement. We also thank Professor Jun Nie and Dr. Yong He of Beijing University of Chemical Technology for their help in RT-FTIR facilities.

References

[1] K. Takada, H.-B. Sun, S. Kawata, Appl. Phys. Lett. 86 (2005) 071122.
[2] S. Kawata, H.-B. Sun, Appl. Surf. Sci. 208–209 (2003) 153–158.
[3] S. Wu, J. Serbin, M. Gu, J. Photochem. Photobiol. A: Chem. 181 (2006) 1–11.
[4] B.H. Cumpston, S.P. Ananthavel, S. Barlow, D.L. Dyer, J.E. Ehrlich, L.L. Erskine, A.A. Heikal, S.M. Kuebler, I.-Y. Sandy Lee, D. McCord-Maughon, J. Qin, H. Röckel, M. Rumi, X. Wu, S.R. Marder, J.W. Perry, Nature 398 (1999) 51–54.
[5] M. Straub, L.H. Nguyen, A. Fazlic, M. Gu, Opt. Mater. 27 (2004) 359–364.
[6] H.-B. Sun, S. Matsuo, H. Misawa, Appl. Phys. Lett. 74 (1999) 786–788.
[7] P. Galajda, P. Ormos, Appl. Phys. Lett. 78 (2001) 249–251.
[8] S. Kawata, H.-B. Sun, T. Tanaka, K. Takada, Nature 412 (2001) 697–698.
[9] K.D. Belfield, X. Ren, E.W.V. Stryland, D.J. Hagan, V. Dubikovsky, E.J. Miesak, J. Am. Chem. Soc. 122 (2000) 1217–1218.
[10] C. Li, L. Luo, S. Wang, W. Huang, Q. Gong, Y. Yang, S. Feng, Chem. Phys. Lett. 340 (2001) 444–448.
[11] M. Farsari, G. Filippidis, K. Sambani, T.S. Drakakis, C. Fotakis, J. Photochem. Photobiol. A: Chem. 181 (2006) 132–135.
[12] K.J. Schafer, J.M. Hales, M. Balu, K.D. Belfield, E.W. Van Stryland, D.J. Hagan, J. Photochem. Photobiol. A: Chem. 162 (2004) 497–502.
[13] D.P. Specht, P.A. Martic, S. Farid, Tetrahedron 38 (1982) 1203–1211.
[14] B.M. Monroe, G.C. Weed, Chem. Rev. 93 (1993) 435–448.
[15] J.L.R. Williams, D.P. Specht, S. Farid, Polym. Eng. Sci. 23 (1983) 1022–1024.
[16] J.P. Fouassier, F. Morlet-Savary, K. Yamashita, S. Imahashi, J. Appl. Polym. Sci. 62 (1996) 1877–1885.
[17] J.P. Fouassier, F. Morlet-Savary, Polymer 38 (1997) 1415–1421.
[18] J.P. Fouassier, D. Ruhlmann, B. Graff, Y. Takimoto, M. Kawabata, M. Harada, J. Imaging Sci. Technol. 37 (1993) 208–210.
[19] X. Allonas, J.P. Fouassier, M. Kaji, M. Miyasaka, T. Hidaka, Polymer 42 (2001) 7627–7634.
[20] Y. Zhao, X. Li, F. Wu, X. Fang, J. Photochem. Photobiol. A: Chem. 177 (2006) 12–16.
[21] X. Li, Y. Zhao, T. Wang, M. Shi, F. Wu, Dyes Pigments 74 (2007) 108–112.
[22] J.N. Demas, G.A. Crosby, J. Phys. Chem. 75 (1971) 991–1024.
[23] C. Xu, W.W. Webb, J. Opt. Soc. Am. B 13 (1996) 481–491.
[24] J.R. Lakowicz, Principles of Fluorescence Spectroscopy, 2nd ed., Kluwer Academic/Plenum Publisher, New York, 1999.
[25] B.R. Cho, K.H. Son, S.H. Lee, Y.-S. Song, Y.-K. Lee, S.-J. Jeon, J.H. Choi, H. Lee, M. Cho, J. Am. Chem. Soc. 123 (2001) 10039–10045.
[26] T.-C. Lin, G.S. He, P.N. Prasad, L.-S. Tan, J. Mater. Chem. 14 (2004) 982–991.
[27] O. Mongin, L. Porrès, L. Moreaux, J. Mertz, M. Blanchard-Desce, Org. Lett. 4 (2002) 719–722.
[28] Y. Lu, F. Hasegawa, T. Goto, S. Ohkuma, S. Fukuhara, Y. Kawazu, K. Totani, T. Yamashita, T. Watanabe, J. Mater. Chem. 14 (2004) 75–80.
[29] A. Fischer, C. Cremer, E.H.K. Stelzer, Appl. Opt. 34 (1995) 1989–2003.
[30] P.J. Campagnola, D.M. Delguidice, G.A. Epling, K.D. Hoffacker, A.R. Howell, J.D. Pitts, S.L. Goodman, Macromolecules 33 (2000) 1511–1513.
[31] J.V. Crivello, M. Jang, J. Photochem. Photobiol. A: Chem. 159 (2003) 173–188.
[32] J.V. Crivello, S. Kong, J. Polym. Sci. Part A: Polym. Chem. 38 (2000) 1433–1442.
[33] Z. Gomurashvili, J.V. Crivello, J. Polym. Sci. Part A: Polym. Chem. 39 (2001) 1187–1197.
[34] J.W. Stansbury, S.H. Dickens, Dental Mater. 17 (2001) 71–79.
[35] W.H. Teh, U. Dürig, G. Salis, R. Harbers, U. Drechsler, R.F. Mahrt, C.G. Smith, H.-J. Güntherodt, Appl. Phys. Lett. 84 (2004) 4095–4097.